# Effect of Plasma Treatment on the Sensor Properties of a Light-Addressable Potentiometric Sensor (LAPS)

*Dua Özsoylu, Sefa Kizildag, Michael J. Schöning, and Torsten Wagner\**

A light-addressable potentiometric sensor (LAPS) is a field-effect-based (bio-) chemical sensor, in which a desired sensing area on the sensor surface can be defined by illumination. Light addressability can be used to visualize the concentration and spatial distribution of the target molecules, e.g., $H^+$ ions. This unique feature has great potential for the label-free imaging of the metabolic activity of living organisms. The cultivation of those organisms needs specially tailored surface properties of the sensor. $O_2$ plasma treatment is an attractive and promising tool for rapid surface engineering. However, the potential impacts of the technique are carefully investigated for the sensors that suffer from plasma-induced damage. Herein, a LAPS with a $Ta_2O_5$ pH-sensitive surface is successfully patterned by plasma treatment, and its effects are investigated by contact angle and scanning LAPS measurements. The plasma duration of 30 s (30 W) is found to be the threshold value, where excessive wettability begins. Furthermore, this treatment approach causes moderate plasma-induced damage, which can be reduced by thermal annealing (10 min at 300 °C). These findings provide a useful guideline to support future studies, where the LAPS surface is desired to be more hydrophilic by $O_2$ plasma treatment.

## 1. Introduction

Potentiometric sensors based on a semiconductor-insulator field-effect structure play an important role in label-free (bio-)chemical

D. Özsoylu, Prof. S. Kizildag
Medical Biology and Genetics
Graduate School of Health Sciences
Dokuz Eylül University
Balcova, 35340 Izmir, Turkey

D. Özsoylu, Prof. M. J. Schöning, Prof. T. Wagner
Institute of Nano- and Biotechnologies
Aachen University of Applied Sciences
Heinrich-Mußmann-Straße 1, 52428 Jülich, Germany
E-mail: torsten.wagner@fh-aachen.de

The ORCID identification number(s) for the author(s) of this article can be found under https://doi.org/10.1002/pssa.201900259.

sensing.[1] The light-addressable potentiometric sensor (LAPS) is an important subtype of this kind of sensors, which is able to detect the variations of the surface charge in a spatially resolved manner.[2] **Figure 1** provides an overview of the working principle of a pH-sensitive $Ta_2O_5$ LAPS. Depending on the concentration of the $H^+$ ions in the analyte solution, a surface potential is generated on the transducer, superimposed with the DC bias voltage applied between a reference electrode and the semiconductor. Therefore, this generates a space-charge region at the semiconductor/insulator interface. A modulated light source is used to create electron-hole pairs by illuminating a certain area of the LAPS structure. The local interaction of those electron-hole pairs with the space-charge region provides an externally detectable photocurrent. Local variations in the surface potential influence the amplitude of the photocurrent in the space-charge region. In this way, by changing the location of the light source, the generated photocurrent in the particular sensor area can be read out.[1–5]

Typical current versus voltage plots (I/V curves) can be obtained by sweeping the applied bias voltage and simultaneously illuminating an area of the semiconductor. As shown in Figure 1b, depending on the local analyte concentration in the solution, the I/V curve moves along the horizontal axis. When the photocurrent (e.g., at the inflection point of the slope) is defined as constant, the horizontal shift $\Delta V$, which corresponds to the local change of the potential at this particular measurement area, can be calculated as a function of time (Figure 1c). More details regarding the measurement principle can be found elsewhere.[1,3,6]

The spatial scanning principle of the LAPS also has a great potential for chemical imaging applications, especially where biological substances such as animal cells or microorganisms are concerned. The metabolic activity of the cultured cells on the sensor surface can be detected by means of marker molecules such as $H^+$ ions at the interface between the sensor surface and the cells. This concept has an additional benefit in the biological imaging because this investigating area is usually not accessible to other methods, which provides a label-free concept.[3]

Nonthermal plasma treatment offers an attractive and promising tool for a rapid, low-cost, and environmental friendly surface engineering. It is increasingly used in sensor applications
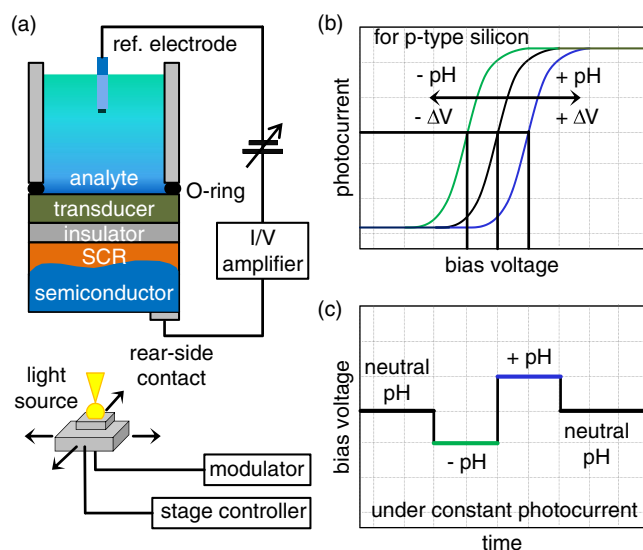
**Figure 1.** a) Schematic representation of the scanning LAPS measurement setup with a light-addressable potentiometric sensor (LAPS), electrical connection, and light source; SCR, space-charge region. b) Schematic I/V curves of the LAPS structure for different analyte concentrations. c) Schematic drawing of constant photocurrent mode measurement of the LAPS structure for different analyte concentrations; ref.: reference.

for surface activation, etching, decontamination, and deposition. For instance, oxygen ($O_2$) plasma was used successfully to remove organic capping agents from gold nanoparticles on a field-effect $SiO_2$ EIS (electrolyte-insulator-semiconductor) sensor.[7] It was also found to be effective in surface functionalization to improve the immobilization of enzymes on $SiO_2$ EIS sensors.[7] In another study where a $Si_3N_4$ EIS sensor was used, $O_2$ plasma treatment was reported as a useful tool for both improving the enzyme immobilization and increasing the pH sensitivity.[8]

In addition, the plasma treatment is an excellent tool to improve bio-compatibility of surfaces by controlling the surface wettability.[9] It is well known that most animal cells tend to prefer rather hydrophilic surfaces but not superhydrophilic surfaces (contact angle below 5°) for growth, adhesion, and spread,[10–13] despite some exceptions.[14] A sufficient adsorption of proteins to the surface is crucial to mediate the adhesion of cells in cell culture medium. However, proteins are unable to adhere to superhydrophilic surfaces, due to strong repulsive solvation forces arising from strong hydrogen bonding between the water molecules and the surface, which has high surface hydration ability.[9,15]

Other influences of the plasma treatment should be carefully considered: an intensive plasma treatment for a long duration to obtain hydrophilic surfaces adversely influences the electrical properties and the sensing behavior of sensors.[16–19] During the plasma treatment, a plasma-induced damage occurs because of the ion bombardment, radical flux, or radiation emitted by the plasma. In particular, the radiation, e.g., vacuum ultraviolet photons (VUVs), can deeply penetrate the sensor and ionizes atoms of the semiconductor lattice and dielectric layer, resulting in imparities and hence a change of the electrical behavior of the

sensor.[16–19] Because of all of these, characterization and optimization of plasma treatment play an important role in this field. However, the studies to date tended to focus on $SiO_2$ EIS sensors[7,8,19,20] rather than $Ta_2O_5$ LAPS. In a study that set out to improve the $Na^+$-ion sensitivity of a $HfO_2$ LAPS, the thermal (300 °C) carbon tetrafluoride ($CF_4$) plasma treatment was utilized.[21] In another study from the same group, this treatment was used again to increase ammonium ($NH_4^+$) ion sensitivity of a $HfO_2$ LAPS.[22] However, no previous studies investigated the effects of $O_2$ plasma treatment on $Ta_2O_5$ LAPS in terms of wettability for cell culturing and effect toward the signal properties.

In this study, the influence of $O_2$ plasma treatment and thermal annealing on $Ta_2O_5$ LAPS were investigated by means of contact angle- and scanning LAPS measurements. Furthermore, this article seeks to address the following questions: 1) What is the optimum $O_2$ plasma treatment duration for the LAPS that can provide high hydrophilic properties, but does not impact the sensor signal? 2) Is there a correlation between the measurement signal and the wettability alterations when the sensor is incubated in cell culture medium? 3) Is there an optimum condition for the plasma treatment, which emphasizes the incubation of cell culture medium and having no negative impact on the sensor characteristics?

## 2. Experimental Section

### 2.1. Fabrication of the LAPS Chip

The LAPS consisted of a p-doped silicon wafer (400 μm, <100>, 5–10 Ωcm) and a 30 nm thick $SiO_2$ layer prepared by thermal dry oxidation. Electron-beam evaporation technique was utilized to deposit an additional layer of 30 nm tantalum on top of the $SiO_2$ layer. After a thermal oxidation step (520 °C, 120 min), a 60 nm thick $Ta_2O_5$ layer was achieved. To create an ohmic rear-side contact, the $SiO_2$ layer on the backside of the silicon wafer was removed by hydrofluoric acid (HF), and an aluminum layer with a thickness of 300 nm was deposited by electron-beam evaporation. The annealing (10 min, 400 °C in $N_2$ atmosphere) was carried out to improve the connection between the aluminum and the silicon wafer. The wafer was diced into single chips with the size of $20 \times 20$ mm$^2$. The rear-side contact was partially detached by an HF etching step to create an illumination window ($15 \times 15$ mm$^2$) to enable illumination from the light source.

### 2.2. Contact Angle Measurements

Water contact angle measurements were carried out by a sessile drop technique (static) using an optical contact angle measuring device (DataPhysics Instruments GmbH, Germany). The measurement involved adding 5 μl of de-ionized water drops in a minimum of three randomly selected spots across the sensor surfaces. Images were acquired 10 s after drop impact, and contact angles were calculated by using the software module (SCA 20) of the device. The controlled environment temperature was 22 °C, and the relative humidity was 58%–60%. Three LAPS chips were used for each experimental group. Hydrophobic recovery experiments consisted of five different parameter

settings (15 chips), whereas annealing experiments consisted of treated (3 chips) and control samples (3 chips). Before the measurements, the samples were rinsed with de-ionized water and dried with nitrogen. After the last culture medium incubation step in the experiments about hydrophobic recovery, the samples were in addition cleaned in an ultrasonic bath using consecutively acetone, isopropanol, ethanol, and de-ionized water for 3 min.

### 2.3. Plasma Treatment

To see the effects of plasma treatment on wettability and hydrophobic recovery, the LAPS chips ($n = 21$) were subjected to $O_2$ plasma treatment using a low-pressure plasma system from Diener Plasma Surface Technology (model Femto) that was coupled to a radio frequency (RF) generator operating at 40 kHz. $O_2$ gas was injected into the reaction chamber at a controlled pressure of 0.2 mbar and at an excitation power of 30 W, a total gas flow rate of 10 sccm, and plasma exposure durations of 30, 60, 90, and 120 s, respectively. The control samples were masked using a silicon-free adhesive plastic film (model 1007R-6.0, Ultron Systems, Inc., USA) and an aluminum foil on top of it during the plasma treatment (30 s). For scanning LAPS measurements, the right side of the sensor surface was masked during the plasma treatment (30 s).

### 2.4. Scanning LAPS Measurement Setup

The scanning LAPS measurement setup used in this study was described in detail in our previous reports.[1,6,23,24] The schematic diagram of the setup is shown in Figure 1a. In brief, the LAPS chip as described in Section 2.1 was assembled in a measurement cell. An Ag/AgCl electrode with 3 M KCl was used as a reference electrode, which was dipped into the electrolyte solution in the measurement chamber. A movable light-intensity modulated laser (QL78F6S-A from QSI) with a wavelength of 780 nm and a focus point of about 70 μm in diameter was utilized as a light source in the LAPS setup to generate the responsive photocurrent. The motion of the modulated laser in a raster-like manner was precisely controlled by a step motor (GMN, Germany) with stage controller that enables illuminating a certain defined area of the semiconductor.

For the measurement of $I/V$ curves, a bias voltage ranging from $-0.8$ to $+2$ V was applied between the reference electrode and the rear-side contact. The $I/V$ curves were recorded in a scanning manner at 48 different points (24 points on the left side [plasma treatment], 24 points on the right side [reference] of the LAPS) and an average was calculated for the left and right sides separately. This $I/V$ measurement procedure was repeated every 10 min to calculate the corresponding bias voltage at a constant photocurrent of 250 nA. The constant photocurrent measurement graphs were obtained from these data. Titrisol buffer solutions (Titrisol, Merck, Germany) in pH range of 6 to 8 were used as measurement solutions. For incubations and measurements with cell culture medium, a modified Dulbecco's Modified Eagle Medium/Ham's Nutrient Mixture F-12 (DMEM/Ham's F-12, 2:1 mixture, pH 7, without sodium bicarbonate) was prepared with standard culture medium

components such as glucose, glutamine, vitamins, and 5% fetal calf serum (FCS). The chemical images were recorded at a constant bias voltage of 0.5 V that was selected from the middle of depletion range of $I/V$ curve by using either the Titrisol buffer solution (pH 7) or the cell culture medium (pH 7) for incubated samples. The step width of the motors was set to 0.1 mm, and an area of $14 \times 14$ mm$^2$ was scanned, creating a measurement area of $141 \times 141$ measurement spots. The whole measurements were controlled by customized LabVIEW software.

### 2.5. Annealing

A hot plate was used to produce an annealing effect on the LAPS at 300 °C for 10 min. The LAPS was removed from the measurement chamber during the annealing to protect the plastic parts of the chamber. The position of the sensor was marked carefully to reassemble it to the correct location after the annealing.

## 3. Results and Discussion

### 3.1. Effect of Plasma Treatment on Wettability and Hydrophobic Recovery

Liquid wettability indicates hydrophilicity (lower contact angle) and hydrophobicity (higher contact angle) properties of the surfaces. **Figure 2** shows the wettability of plasma-modified $Ta_2O_5$ surfaces investigated with measurements of the contact angle before and after $O_2$ plasma treatment. Overall, the average contact angles of all groups of samples were equal to $62.4° \pm 0.5°$,
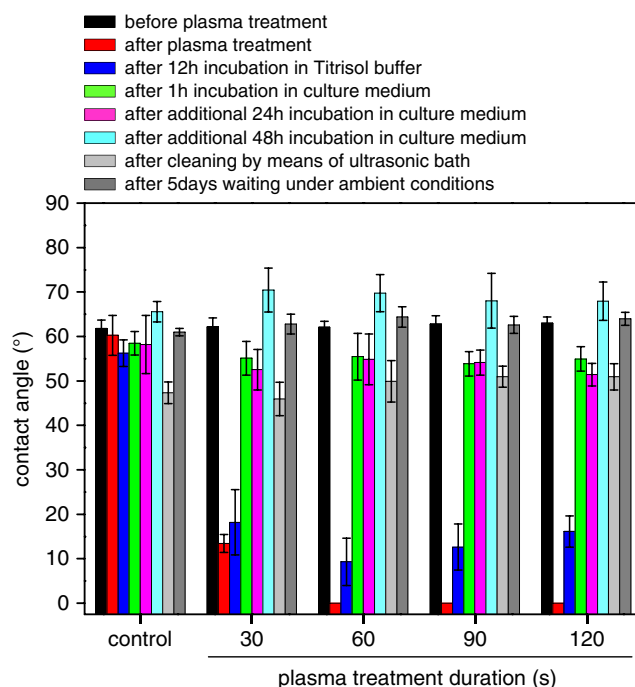


**Figure 2.** Investigation of hydrophilicity alterations and hydrophobic recovery by water contact angles for the series of $O_2$ plasma treatment durations on a $Ta_2O_5$ LAPS; the control corresponds to the sample masked during a plasma treatment for 30 s.

with the given standard deviation margins, before plasma treatment. The hydrophilicity significantly increased for all plasma-treated surfaces except for the control samples, which were, as described, masked during the plasma treatment. This shows that the technique used for masking was effective. For 60–120 s of plasma durations, no contact angle could be recorded because of the extremely high wettability after the treatments. This is indicated in the diagram by the values of "zero" for the respective red bars. On the other hand, for 30 s of plasma duration, the contact angle was reduced to $13.4° \pm 2.0°$ after the treatment.

In addition, after 12 h incubation with Titrisol buffer (pH 7), the samples became more hydrophobic again, except the control samples. For 60–120 s of plasma durations, the contact angle rose to an average of $12.7° \pm 3.7°$, while the contact angle of the sample treated for 30 s rose from $13.4° \pm 2.0°$ to $18.2° \pm 7.3°$. However, the most increase in the contact angle for all plasma durations was seen after the culture medium incubation for 1 h, where the contact angles of all treated surfaces reached an almost equal value of $54.8° \pm 0.7°$ on average and became closer to contact angles of the control samples incubated with the same protocol ($58.5° \pm 2.6°$). This strong wettability decay can be attributed to the adsorption of medium-borne ingredients such as FCS proteins and inorganic matters inside the cell culture medium.[25–27]

An additional medium incubation for 24 h did not lead to any significant changes in the contact angles; however, additional 48 h incubation significantly increased the contact angles in all experimental groups, including the control samples as well. This is probably due to the biological contamination because the incubations were not conducted under sterile environments and some colony traces of microorganisms were seen on the surfaces after additional 48 h of incubation. After the last culture medium incubation step, the samples were cleaned in an ultrasonic bath to remove all surface contaminants. As can be seen in Figure 2, the contact angles in all experimental groups, including the control samples, significantly decreased to $49.0° \pm 2.2°$ on average after the cleaning. This cleaning step emphasizes further that the increase in the contact angles was due to the contaminants, as discussed above. In addition, the average contact angle value, $49.0° \pm 2.2°$ was in complete compliance with the contact angle of clean, bare $Ta_2O_5$ surfaces given in literature.[28] This also proves that the cleaning process was carried out appropriately.

Furthermore, the contact angles for all experimental samples significantly increased from $49.0° \pm 2.2°$ to $62.9° \pm 1.3°$ after waiting for 5 days under room temperature conditions and became equal to their initial values of $62.4° \pm 0.5°$ on average. Such wettability decays are known to be caused by the adsorption of hydrocarbons from the air, minimizing the free surface energy, compared to a recently cleaned surface.[29] Moreover, although they were subjected to in-depth cleaning with an ultrasonic bath, the surfaces did not fully regain their hydrophilicity properties compared to the plasma treatments. This indicates that additional mechanisms are also responsible for the decrease in the surface wettability and surface-free energy with time.

Plasma treatment can generate defective sites like surface-trapped electrons as it was reported for metal oxides.[30,31] These defective sites, which are favorable for hydroxyl adsorption, cause an increase in the surface hydrophilicity. However, after the adsorption of hydroxyl radicals from the medium or air, the surface becomes energetically unstable. This unstable surface gradually loses its hydrophilicity as the previously adsorbed hydroxyl group is replaced gradually by oxygen atoms. This may be the cause of wettability conversion, and this phenomenon can be called "hydrophobic recovery" after plasma treatment on metal oxide.

As described previously (see Section 1), for cell culturing hydrophilic but not superhydrophilic surfaces would be ideal. Because of this, a plasma treatment duration of 30 s was found to be the most ideal. Therefore, this procedure was used for further experiments in this study.

### 3.2. Influence of Plasma Treatment on Characteristics of the LAPS

**Figure 3** shows $I/V$ curves before and after plasma treatment. The sensor responses toward varying pH buffer solutions, the effect of plasma treatment, and the response to culture medium are schematically shown in **Figure 4**. The measurements for both control and treatment groups were performed at the same time using only one sensor due to spatial resolution ability of the LAPS. First, an average voltage difference of 16 mV was found between the left side (L, treated) and right side (R, control) of the sensor. The plasma treatment (30 s) was applied after 11 h and 15 min sensor operation. After the treatment, the treated side of the sensor showed an average increase of about 250 mV in the sensor signal although the masked side showed an average increase of about 17 mV. The sensor signal from the masked side of the sensor exhibited a high reproducibility, quite low hysteresis ($\approx 4$ mV), and very low drift (0.034 mV h$^{-1}$) within a measurement time for 117 h. In addition, a negative drift of 1.18 mV h$^{-1}$ in the treated side of the sensor was observed after the plasma treatment. **Figure 5** shows the pH sensitivity of the
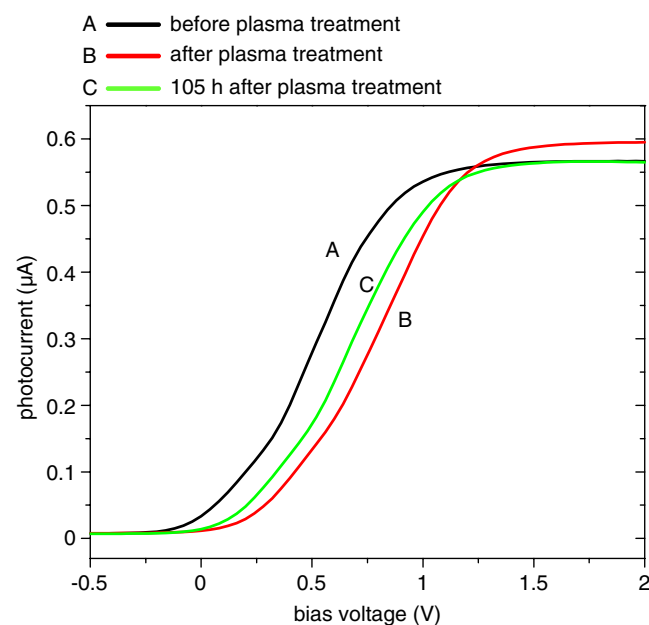


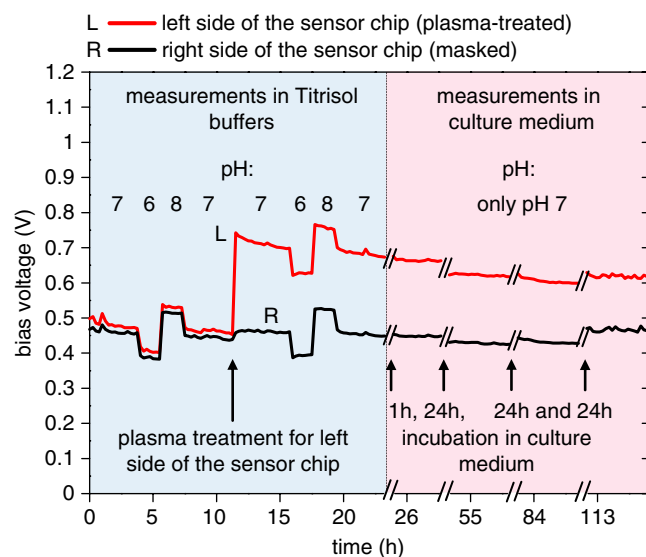**Figure 3.** I/V curves of the LAPS structure before and after plasma treatment.

**Figure 4.** Constant photocurrent measurement of the left (L) and right (R) sides of the LAPS before and after $O_2$ plasma treatment (30 s). The right side was masked during the plasma treatment.
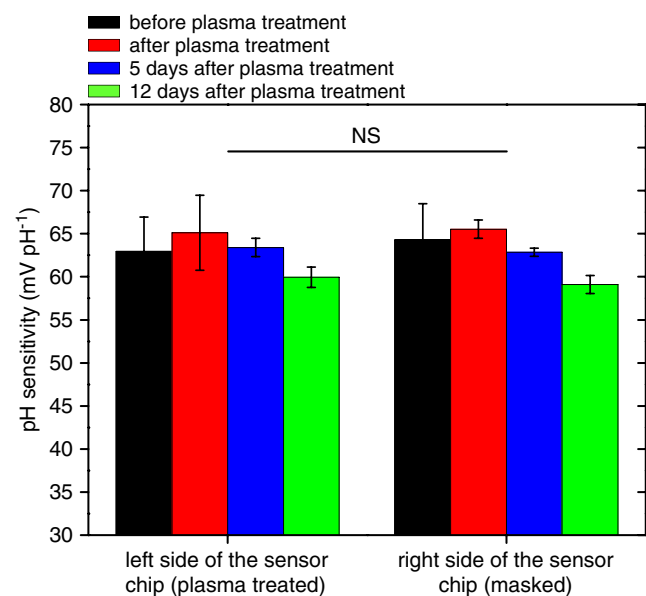


**Figure 5.** pH sensitivity before and after $O_2$ plasma treatment (30 s); NS, not significant, $p > 0.05$ (unpaired, two-tailed t-test).

treated side and the masked side of the sensor before and after plasma treatment. The data here were obtained from the results of the measurements shown in Figure 4, and after these measurements, the sensor was left inside the medium until the measurement was continued 5 and 12 days after the plasma treatment (not shown in Figure 4). Each measurement for pH sensitivity was performed by using Titrisol buffer solutions in the range of pH 6–pH 8. According to the results, the differences in pH sensitivity were not statistically significant between the two groups, the left side (treated) and the right side (masked) of the

sensor ($p = 0.96$, unpaired, two-tailed t-test). However, the standard deviations of the results on the treated side of the sensor were higher than those of the masked side after the plasma treatment but they became smaller and closer to each other 5 and 12 days after the plasma treatment, respectively. In addition, the pH sensitivities of both sides were slightly higher than the theoretical value of maximum Nernstian sensitivity (59.6 mV pH$^{-1}$ at 300 K). This might be explained by temperature fluctuations of the laboratory during the measurements, an increase in the surface site density,[32] and insufficient concentration diversity (only pH 6, pH 7, and pH 8) of buffer solutions used for calibrating the pH sensitivity.

In addition, as it can be noticed in Figure 4, the exposure for 1 h to the cell culture medium after the plasma treatment did not influence the sensor signal although it caused the described increase in the contact angles of the plasma-treated sensors (see Section 3.1). To further study these effects, chemical images were recorded at a constant bias voltage of 0.5 V. With the help of those images, one can reveal the spatial distributions of the photocurrent signal and hence visualize the influences due to masking, plasma treatment, annealing, or medium incubation. To create such a chemical image, 19 881 different measurement points on the sensor were recorded separately, and results were shown as a chemical image to indicate the location, strength, and uniformity of said influences. The results were summarized in **Figure 6**.

Overall, as it can be seen from the chemical images (Figure 6), the treated side (L) of the sensor showed a remarkable decrease in the photocurrents after the plasma treatment although the masked side (R) remained almost the same. Thereafter, the medium incubation did not cause any significant changes in both sides regarding the photocurrents despite the increase in the contact angle of the treated side of the sensor (see Figure 2). Furthermore, the treated side depicts a slight drift in the photocurrents in comparison to the masked side. This can be seen by the change of color between "1 h and 48 h" in the left lower corner of the chemical images. All of these were in agreement with previous results for individual I/V measurements discussed earlier in this section. In addition, the images present a homogeneous spatial distribution of the photocurrents along the sensor, which indicates the uniform influences of the plasma treatment.

These results show that the $O_2$ plasma treatment affects not only the surface wettability property but also the sensor characteristics. In addition, after plasma treatment, the wettability decay does not correlate to the recovery of sensor characteristics, as both depend on different parameters.

The radiation, especially VUVs, can inject electrons and/or electron-hole pairs in the semiconductor and dielectric layers. They are able to move throughout the layer and become trapped, recombine, or leave the layers.[16–19] The trapped charges within the dielectric layer can contribute to the decreased photocurrent signal after the plasma treatment. Neutralization of the charge accumulation over time by leakage currents under the electrical field can be the reason for the drift, which was seen in the treated side (L) of the sensor. In a previous study, a large drift of 27 mV min$^{-1}$ and a voltage shift of 1710 mV were reported after a SiO$_2$ surface of an EIS sensor was treated by $O_2$ plasma for 2 min at 100 W.[20] In this study, a more gentle condition
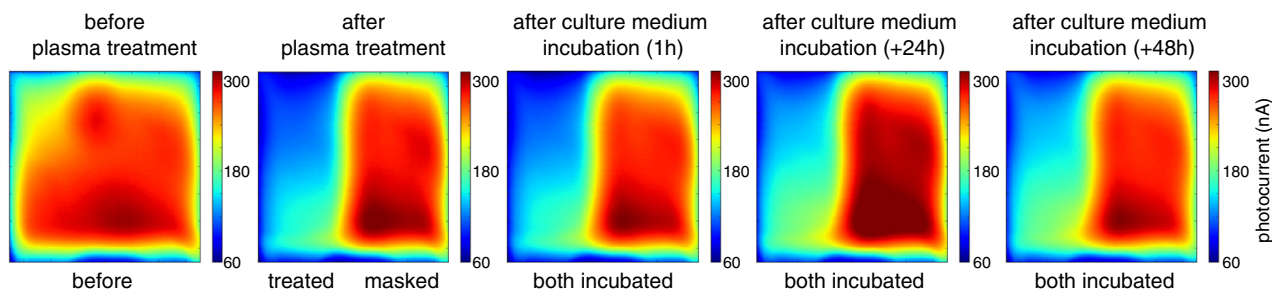
**Figure 6.** Chemical images from the scanning LAPS setup under $O_2$ plasma treatment (30 s) and various incubation procedures. The right side (R) of the LAPS was masked during the plasma treatment, and the mask was removed right after that. The treatment regimes were performed sequentially according to the order in the images on the same LAPS. The size of each image is $14 \times 14 \, mm^2$. Cell culture medium with FCS and L-glutamine and without sodium bicarbonate was used for each incubation. The pH values of the measurement solutions were always adjusted to pH 7.

(30 s, 30 W) was selected for the plasma treatment to reduce the drift and the average potential shifts, which were seen to be $1.18 \, mV \, h^{-1}$ and 250 mV, respectively. Usually, a drift of this size can be acceptable for cell culture experiments, especially as it appears to be uniform along the sensor surface, which can therefore be compensated by means of the differential measuring principle of the LAPS.[2]

### 3.3. Annealing Effect on the Sensor Properties of the LAPS

For constant photocurrent mode measurement, the recorded signals from the left side (L, treated) and the right (R, control) side of the sensor were plotted in **Figure 7**. After the plasma treatment step for 30 s, the treated side of the sensor showed an average increase of about 210 mV in the bias voltage signal although the masked side showed an average decrease of about 2 mV. After the described annealing step (10 min at 300 °C), the bias
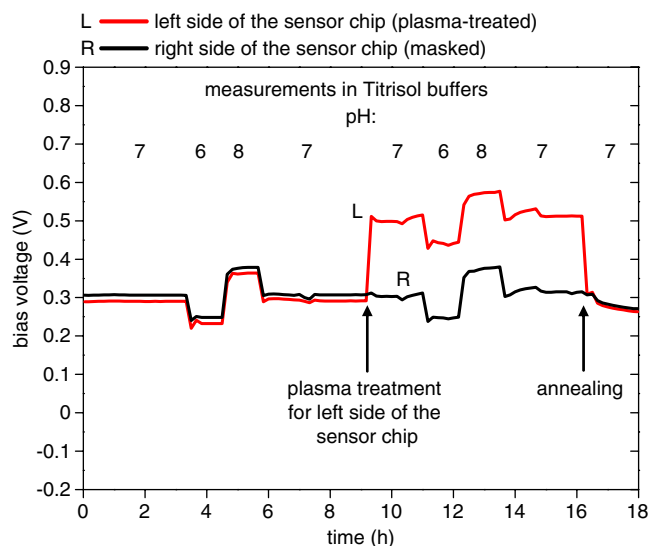
voltage signal from the treated side of the sensor returned to its initial value. In addition, the differences in pH sensitivity were not statistically significant between the two groups, the left side (treated) and the right side (masked) of the sensor ($p = 0.65$, unpaired, two-tailed $t$-test).

**Figure 8** displays the chemical images and the wettability alterations, response to the plasma treatment (30 s), and the annealing (10 min, 300 °C). As it can be seen from the chemical images (Figure 8a), the left side of the sensor showed a remarkable decrease in the photocurrent after the plasma treatment despite the fact the masked side remained the same. This is consistent with the results in Section 3.2. After the annealing process, the treated side of the sensor depicts an increase of the photocurrent and went almost completely back to its initial value. This might be explained by the release of the trapped charges from the dielectric material, as the increased temperature will accelerate those equilibrium processes.[19,20] In addition, the images present a homogeneous spatial distribution of the photocurrents among the sensor surface, which indicates an uniform plasma treatment and annealing process.

In addition, the hydrophilicity significantly increased for the treated side of the sensor except for the control side, which was masked during the plasma treatment. The annealing process changed the wettability properties of both sides and brought them closer to the contact angle values (49°) of a bare $Ta_2O_5$ surface (Figure 8b). The increase of the contact angle in the treated side (L) might be due to an accelerated hydrophobic recovery at a higher temperature. On the other hand, the removal of contaminants at 300 °C could explain the decrease in the contact angle on the control side of the sensor.

These results underline that an annealing process (10 min, 300 °C) has the ability to completely "reset" the properties of the LAPS regarding its surface wettability and electrochemical characteristic. This is essential to provide a good reusability of LAPS. Moreover, the results indicate that an annealing step could be utilized to reset a plasma-patterned LAPS.



**Figure 7.** Constant photocurrent measurement of the left (L) and right (R) sides of the LAPS shows the effect of an annealing (10 min, 300 °C) procedure on the $O_2$ plasma-treated part (L) and nontreated part (R) of the LAPS. The plasma treatment was performed after 9 h and 10 min sensor operation. The annealing step was set at 16 h and 10 min.

## 4. Conclusions

In this study, the effects of $O_2$ plasma treatment and annealing on a $Ta_2O_5$ LAPS were investigated by means of contact
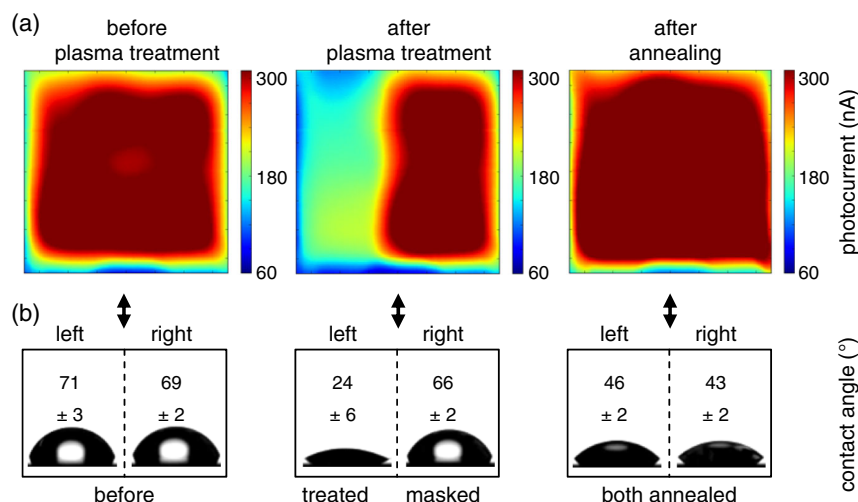
**Figure 8.** a) Chemical images from the scanning LAPS setup before and after $O_2$ plasma treatment (30 s) and annealing (10 min, 300 °C) of a $Ta_2O_5$-based LAPS. The treatments were performed sequentially according to the order in the images on the same LAPS. The size of each image is $14 \times 14$ mm². b) Representative images of sessile water droplets on left (L) and right (R) sides of the LAPS with a $Ta_2O_5$ surface, and the corresponding measured static contact angles.

angle- and scanning LAPS measurements. The conclusions are summarized as follows.

The technique used for masking against the effects of the plasma treatment was effective, simple, and low cost. It successfully preserved both wettability and electrical properties of the sensor. The 30 s of plasma duration (30 W) was found to be a threshold value where the excessive wettability, being superhydrophilic, begins. To determine this transition was particularly important since most animal cells tend to prefer rather hydrophilic surfaces but not superhydrophilic surfaces (contact angle below 5°) for culturing.

After the plasma treatment, an increase of about 250 mV in the bias voltage signal was observed in the treated side of the sensor; this was also confirmed by means of chemical images. This might be associated with the radiation emitted by plasma, especially VUV, which can inject electrons and/or electron-hole pairs in the dielectric layer. The cell culture medium incubation after plasma treatment did not cause any changes in the photocurrent response of the sensor; however, it led to strong wettability decays most likely due to the adsorption of serum proteins in the medium. This affinity of the surface for proteins could be utilized to modify the surface with specific proteins. A thermal annealing process of 10 min at 300 °C led to a "reset" of the LAPS properties regarding its altered surface wettability and electrochemical characteristic. This behavior enables the reusability of the LAPS chip. Furthermore, thermal sterilization of the sensor can be performed, which is an important process step in cell culture experiments.

These findings provide a useful guideline to support future studies, e.g., determining the metabolic activity of cells, where the LAPS surface is desired to be more hydrophilic by $O_2$ plasma treatment. In addition, these findings can be applied to other types of field-effect bio-sensors like EIS (electrolyte-insulator-semiconductor) or ISFET (ion-sensitive field-effect transistor), which has $Ta_2O_5$ surface. These could be the subject of future studies.

## Conflict of Interest

The authors declare no conflict of interest.

[1] T. Yoshinobu, S. Krause, K. I. Miyamoto, C. F. Werner, A. Poghossian, T. Wagner, M. J. Schöning, *(Bio-)Chemical Sensing and Imaging by LAPS and SPIM*, Springer International Publishing, Cham **2018**, pp. 103–132.

[2] S. Dantism, D. Röhlen, T. Wagner, P. Wagner, M. J. Schöning, *Phys. Status Solidi A* **2018**, *215*, 1800058.

[3] F. Wu, I. Campos, D. W. Zhang, S. Krause, *Proc. Royal Soc. A* **2017**, *473*, 20170130.

[4] M. J. Schöning, T. Wagner, C. Wang, R. Otto, T. Yoshinobu, *Sens. Actuators B: Chem.* **2005**, *108*, 808.

ADVANCED
SCIENCE NEWS

www.advancedsciencenews.com

physica pssa
status solidi

www.pss-a.com

[5] T. Wagner, C. Rao, J. Kloock, T. Yoshinobu, R. Otto, M. Keusgen, M. J. Schöning, *Sens. Actuators B: Chem.* **2006**, *118*, 33.

[6] A. Poghossian, T. Yoshinobu, A. Simonis, H. Ecken, H. Lüth, M. J. Schöning, *Sens. Actuators B: Chem.* **2001**, *78*, 237.

[7] J. Gun, D. Rizkov, O. Lev, M. H. Abouzar, A. Poghossian, M. J. Schöning, *Microchim. Acta* **2009**, *164*, 395.

[8] L.-T. Yin, J.-C. Chou, W.-Y. Chung, T.-P. Sun, S.-K. Hsiung, *IEEE Trans. Biomed. Eng.* **2001**, *48*, 340.

[9] L. Chen, C. Yan, Z. Zheng, *Mater. Today* **2018**, *21*, 38.

[10] K. Fukazawa, A. Nakao, M. Maeda, K. Ishihara, *ACS Appl. Mater. Interfaces* **2016**, *8*, 24994.

[11] K. Webb, V. Hlady, P. A. Tresco, *J. Biomed. Mater. Res.* **1998**, *41*, 422.

[12] J. T. Jeong, M.-K. Choi, Y. Sim, J. T. Lim, G. S. Kim, M. J. Seong, J. H. Hyung, K. Soo Kim, A. Umar, S. K. Lee, *Sci. Rep.* **2016**, *6*, 33835.

[13] S. Mi Baek, M. Hwan Shin, J. Moon, H. Sang Jung, S. Am Lee, W. Hwang, J. T. Yeom, S. Kwang Hahn, H. Kim, *Sci. Rep.* **2017**, *7*, 44213.

[14] S. Shin, J. Seo, H. Han, S. Kang, H. Kim, T. Lee, *Materials* **2016**, *9*, 116.

[15] M. Ahmed, T. Ramos, F. Damanik, B. Quang, P. Wieringa, M. Bennink, C. van Blitterswijk, J. Boer, L. Moroni, *Sci. Rep.* **2015**, *5*, 14804.

[16] L. Shohet, H. Ren, M. Nichols, H. Sinha, W. Lu, K. Mavrakakis, Q. Lin, N. M. Russell, M. Tomoyasu, G. Antonelli, *Proc. SPIE* **2012**, *8328*, 83280I.

[17] J. L. Lauer, G. S. Upadhyaya, H. Sinha, J. B. Kruger, Y. Nishi, J. L. Shohet, *J. Vac. Sci. Technol. A* **2012**, *30*, 01A109.

[18] M. Hasumi, J. Takenezawa, T. Nagao, T. Sameshima, *Jpn. J. Appl. Phys.* **2011**, *50*, 03CA03.

[19] A. Szekeres, S. Alexandrova, K. Kirov, *Phys. Status Solidi A* **1980**, *62*, 727.

[20] J. Arreola, M. Keusgen, M. J. Schöning, *Phys. Status Solidi A* **2017**, *214*, 1700025.

[21] C. H. Chin, T. F. Lu, J. C. Wang, J. H. Yang, C. E. Lue, C. M. Yang, S. S. Li, C. S. Lai, *Jpn. J. Appl. Phys.* **2011**, *50*, 04DL06.

[22] J. H. Yang, T. F. Lu, J. C. Wang, C. M. Yang, D. G. Pijanowska, C. H. Chin, C. E. Lue, C. S. Lai, *Sens. Actuators B: Chem.* **2013**, *180*, 71.

[23] T. Yoshinobu, H. Ecken, A. M. Ismail, H. Iwasaki, H. Lüth, M. J. Schöning, *Electrochim. Acta* **2001**, *47*, 259.

[24] W. Moritz, T. Yoshinobu, F. Finger, S. Krause, M. Martin-Fernandez, M. J. Schöning, *Sens. Actuators B: Chem.* **2004**, *103*, 436.

[25] B. Kasemo, J. Lausmaa, *J. Biomed. Mater. Res.* **1988**, *22*, 145.

[26] C. C. Wu, C. K. Wei, C. C. Ho, S. J. Ding, *Materials* **2015**, *8*, 684.

[27] V. Cimalla, *Label-Free Biosensors Based on III-Nitride Semiconductors*, Springer, Cham **2018**, pp. 59–102.

[28] N. Donkov, A. Zykova, V. Safonov, E. Mateev, *Probl. Atom. Sci. Tech.* **2009**, *1*, 153.

[29] D. Kara, L. A. Belyaeva, L. Jiang, L. M. C. Lima, G. F. Schneider, *Nat. Commun.* **2018**, *9*, 4185.

[30] D. P. Subedi, D. K. Madhup, A. Sharma, U. M. Joshi, A. Huczko, *Int. Nano Lett.* **2012**, *2*, 1.

[31] R. D. Sun, A. Nakajima, A. Fujishima, T. Watanabe, K. Hashimoto, *J. Phys. Chem. B* **2001**, *105*, 1984.

[32] T. M. Pan, C. W. Wang, C. Y. Chen, *Sci. Rep.* **2017**, *7*, 2945.